American Diabetes Association. diabetes

Altered phenotype of β-cells and other pancreatic cell lineages in patients with diffuse Congenital Hyperinsulinism in Infancy due to mutations in the ATP-sensitive K-channel

Journal:	*Diabetes*
Manuscript ID:	DB14-1202.R2
Manuscript Type:	Brief Report
Date Submitted by the Author:	n/a

Complete List of Authors:	Salisbury, Rachel; University of Manchester, Centre for Endocrinology & Diabetes Han, Bing; University of Manchester, Faculty of Life Sciences Jennings, Rachel; University of Manchester, Centre for Endocrinology & Diabetes; Central Manchester University Hospitals NHS Foundation Trust, Endocrinology Department Berry, Andrew; University of Manchester, Centre for Endocrinology & Diabetes Stevens, Adam; Central Manchester University Hospitals NHS Foundation Trust, Endocrinology Department Mohamed, Zainab; University of Manchester, Faculty of Life Sciences; central Manchester University Hospitals NHS Foundation Trust, Paediatric Endocrinology Sugden, Sarah; University of Manchester, Centre for Endocrinology & Diabetes De Krijger, Ronald; Erasmus MC, University Medical Centre; Reinier de Graaf Hospital, Department of Pathology Cross, Sarah; University of Oxford, Nuffield department of surgical sciences and Oxford centre for Diabetes Johnson, Paul; University of Oxford, Nuffield department of surgical sciences and Oxford centre for Diabetes Newbould, Melanie; Central Manchester University Hospitals NHS Foundation Trust, Paediatric histopathology Cosgrove, Karen; University of Manchester, Faculty of Life Sciences Piper Hanley, Karen; University of Manchester, Centre for Endocrinology & Diabetes Banerjee, Indraneel; University of Manchester, Centre for Endocrinology & Diabetes; Central Manchester University Hospitals NHS Foundation Trust, Paediatric Endocrinology Dunne, Mark; University of Manchester, Faculty of Life Sciences Hanley, Neil; University of Manchester, Endocrinology & Diabetes

BRIEF REPORT

Altered phenotype of β-cells and other pancreatic cell lineages in patients with diffuse Congenital Hyperinsulinism in Infancy due to mutations in the ATP-sensitive K-channel

[Short running title: Pancreatic cell abnormalities in diffuse CHI**]**

Rachel J. Salisbury[1], Bing Han[2], Rachel E Jennings [1,3], Andrew A. Berry[1], Adam Stevens[2,4], Zainab Mohamed[2,4], Sarah A. Sugden[1], Ronald De Krijger[5,6], Sarah E. Cross[7], Paul P.V. Johnson[7], Melanie Newbould[8], Karen E. Cosgrove[3], Karen Piper Hanley[1], Indraneel Banerjee[1,4], Mark J. Dunne[2*], Neil A. Hanley[1,3*]

1. Centre for Endocrinology and Diabetes, Institute of Human Development, Faculty of Medical & Human Sciences, Manchester Academic Health Sciences Centre, University of Manchester, Oxford Rd, Manchester, M13 9PT, UK.
2. Faculty of Life Sciences, University of Manchester, Oxford Rd, Manchester M13 9PT, UK.
3. Endocrinology Department, Central Manchester University Hospitals NHS Foundation Trust, Oxford Rd, Manchester, M13 9PT, UK.
4. Paediatric Endocrinology, Central Manchester University Hospitals NHS Foundation Trust (CMFT), Oxford Rd, Manchester, M13 9PT, UK.
5. Erasmus MC, University Medical Center, Rotterdam, The Netherlands
6. Dept. of Pathology, Reinier de Graaf Hospital, Delft, The Netherlands
7. DRWF Human Islet Isolation Facility, Nuffield Department of Surgical Sciences and Oxford Centre for Diabetes, Endocrinology and Metabolism, University of Oxford, OX3 7LE
8. Paediatric Histopathology, Central Manchester University Hospitals NHS Foundation Trust (CMFT), Oxford Rd, Manchester, M13 9PT, UK

***Addresses for correspondence**

Professors Neil Hanley / Mark Dunne

Centre for Endocrinology & Diabetes

University of Manchester, Oxford Road

Manchester, M13 9PT, UK

Tel: +44 (0)161 275 5281

neil.hanley@manchester.ac.uk / mark.dunne@manchester.ac.uk

Word count: 1,996

Four figures in main text plus an online appendix containing 4 supplementary tables, 1 supplementary video and 8 supplementary figures)

Abstract

Diffuse congenital hyperinsulinism in infancy (CHI-D) arises from mutations inactivating the K_{ATP} channel, however, the phenotype is difficult to explain from electrophysiology alone. Here we have studied wider abnormalities in the β-cell and other pancreatic lineages. Islets were disorganized in CHI-D compared to control. *PAX4* and *ARX* expression was decreased. A tendency to increased *NKX2.2* expression was consistent with its detection in two-thirds of CHI-D δ-cell nuclei, similar to the fetal pancreas and implying immature δ-cell function. CHI-D δ-cells also comprised 10% of cells displaying nucleomegaly. Increased proliferation in CHI-D was most elevated in duct (5-11 fold) and acinar (7-47 fold) lineages. Increased β-cell proliferation observed in some cases was offset by an increase in apoptosis; in keeping with no difference in *INSULIN* expression or surface area stained for insulin between CHI-D and control pancreas. However, nuclear localization of CDK6 and P27 was markedly enhanced in CHI-D β-cells compared to cytoplasmic localization in control cells. These combined data support normal β-cell mass in CHI-D, but with G1/S molecules positioned in favor of cell cycle progression. New molecular abnormalities in δ-cells and marked proliferative increases in other pancreatic lineages indicate CHI-D is not solely a β-cell disorder.

Key words: Human, pancreas, fetal, development, congenital hyperinsulinism, proliferation, β-cells, transcription factor, ATP-sensitive K-channel, KCNJ11, ABCC8

Diffuse congenital hyperinsulinism in infancy (CHI-D) affects the entire pancreas and is characterized by persistent, inappropriate release of insulin in the presence of low blood glucose, commonly accompanied by macrosomia indicating altered intrauterine development (1; 2). In cases where hypoglycaemia necessitates partial or near-total pancreatectomy (1; 2), inactivating mutations in either the *ABCC8* or *KCNJ11* genes, encoding subunits of the K_{ATP} channel, account for approximately 90% of cases (3; 4). These mutations cause persistent β-cell depolarization, inappropriate calcium entry and insulin secretion (5).

Two features of CHI-D imply more diverse pathophysiology. Firstly, some reports have shown increased rates of β-cell proliferation by Ki67, which detects all stages of the cell-cycle except G_0 (6-8). Understanding how CHI-D might promote human β-cell replication is desirable for therapeutic exploitation in diabetes. While the glucose-sensing/insulin-secretion pathway can regulate β-cell proliferation (9) and an intricate array of cell cycle proteins is in place (10), normal human β-cells are recalcitrant in proliferation assays compared to their rodent counterparts (11). Secondly, alterations outside the β-cell lineage imply consequences from abnormal β-cells or that CHI-D directly affects other pancreatic lineages. For instance, pancreatic polypeptide (PP) cells and somatostatin-stained δ-cells have been reported as altered in CHI-D (12). Certainly, K_{ATP} channels are expressed in other islet cell-types and normal β-cell function relies upon multiple intra-islet interactions (5).

Here, we have explored potential defects in differentiation, maturity and proliferation in β-cells and other pancreatic lineages in CHI-D due to mutant K_{ATP} channels.

Research Design and Methods

Human tissue

Pancreatic tissue was received following ethical approval, national codes of practice and informed consent: from ten cases of CHI-D (Supplementary Table 1); or normal control samples as previously described (13). CHI-D was diagnosed from established clinical and histopathological criteria (1; 2), and the identification of *ABCC8* or *KCNJ11* mutations (Supplementary Table 1). Postnatal control cases died from non-pancreatic diagnoses and showed unremarkable pancreatic histology: 2 days-36 months (n=16); ≥12 years (n=4). Fetal control material at 10 to 35 weeks post conception (wpc; n=4) was obtained and processed as described previously (14; 15).

Immunohistochemistry, immunofluorescence and cell counting

Immunohistochemistry and immunofluorescence were performed as described previously (14; 15) (Supplementary Table 2). High-content assessment of $Ki67^+$ cells and $insulin^+$ surface area followed digitization of slides (3D Histech Pannoramic 250 Flash II) using Pannoramic Viewer and HistoQuant software. At least 20 regions of interest were selected (free from connective tissue) and $Ki67^+$ cells calculated as a fraction of the total cell count. No regional differences were measured. Dual-staining of Ki67 and pancreatic lineage markers was assessed from 10 randomly selected fields of view at x200 magnification in at least two positions within each CHI-D or control pancreas, or the entire section (fetal samples; smaller size). Apoptosis combined immunofluorescence for insulin using a conjugated Alexa-Fluor dye (Life Technologies, Paisley, UK) with FITC-labelled terminal deoxynucleotidyl transferase-mediated dUTP-X 3' nick end-labeling (TUNEL) according to the manufacturer's instructions (Trevigen, Gaithersburg, MD, USA). DNase I treatment and omission of the terminal transferase enzyme served as positive and negative controls respectively.

Isolation of RNA, reverse transcription and quantitative PCR

Total RNA was isolated from whole tissue sections using the Qiagen RNeasy FFPE kit protocol according to the manufacturer's instructions. Reverse transcription (RT) and quantitative PCR (qRT-PCR) were performed as described previously using the ΔΔCT method standardized to *HPRT* and *β-ACTIN* and compared to age-matched control (16; 18) (primers in Supplementary Table 3).

Statistical Analysis

Cell counting data are presented as mean ± standard error. Patient and control samples were compared using the Mann-Whitney U test and correlation assessed by the Spearman Rank Correlation test.

Results

Islet structure and hormone colocalization in CHI-D

CHI-D α-cells and δ-cells were more diffusely scattered throughout the islet compared to a peripheral mantle location in early postnatal control tissue (Supplementary Fig. 1A-D; Supplementary Fig. 2A-D). This tended to resolve to match control tissue by the end of the first year, however, overall islet structure remained less organized and compact in CHI-D (Supplementary Fig. 1E-F and Supplementary Fig. 2E-F). In two of the CHI-D samples from early infancy 2-5% of glucagon-positive and insulin-positive cells contained both hormones, similar to fetal pancreas but not observed in any of the postnatal control samples (Supplementary Fig. 3 and video). Co-localization was not observed for insulin with somatostatin, ghrelin, or PP.

'Fetal-like' NKX2.2 in early postnatal CHI-D δ-cells

Given this potential immaturity, we looked for signs of endocrine differentiation in CHI-D. *NEUROG3* detection from whole tissue sections was no higher in CHI-D than age-matched controls and much lower than when fetal NEUROG3-positive cells are most abundant (13) (Fig. 1A). We did not detect convincing NEUROG3 immunoreactivity in CHI-D or age-matched controls

spanning the first year after birth (data not shown). FOXA2 (in β-cells and duct cells), NKX6.1 (β-cells), SOX9 (duct cells) and GATA4 (acinar cells) were all appropriately detected as nuclear proteins in their respective cell-types in CHI-D and age-matched controls (Supplementary Fig. 4 and data not shown). Mean expression of *INSULIN*, *PDX1*, *FOXA2*, *SOX9*, *NKX6.1*, *MAFA* and *MAFB* from whole tissue sections was not altered in CHI-D samples (Fig. 1B). While *NKX2.2* was increased prior to Hochberg correction, *PAX4* and *ARX* were consistently decreased statistically (Fig. 1B; control levels of *NKX2.2* were constant during the first year). This trend towards increased *NKX2.2* in CHI-D reflected cases up to 6 months of age (Fig. 1C). By immunofluorescence in CHI-D, fetal and postnatal control samples nuclear NKX2.2 protein was detected in virtually all β-cells, 80-90% of α-cells and in 75-90% of ghrelin-positive cells. In contrast, NKX2.2 was detected in two-thirds of CHI-D and fetal δ-cells but only in 25% of age-matched control cells (Fig. 1D-E). Given this alteration we examined another feature of CHI-D, nucleomegaly (8; 16). CHI-D islet cells tended to have a slightly larger nucleus than age-matched controls with a clear subset outside a normal distribution showing >50% increase in nuclear diameter (Supplementary Fig. 5A). Most of the cells with these enlarged nuclei stained for insulin and for β-cell transcription factors including NKX6.1 and ISL1 (occasionally PDX1 was missing; Supplementary Fig. 5B). Nucleomegaly was not observed in CHI-D cells positive for glucagon, PP or ghrelin, or in duct or acinar cells (data not shown; Supplementary Fig. 4A and G). However, 10% of nucleomegalic cells contained somatostatin, implying a δ-cell identity (Supplementary Fig. 5C).

Increased cell proliferation in CHI-D is mostly in exocrine cells

Recognizing CHI-D extended beyond β-cells, we studied proliferation in different pancreatic lineages. Total proliferation in control pancreas declined between 10 wpc and 36 months of age (Fig. 2A) with a very low rate from 12 years onwards. During months 1-13 Ki67 count was increased in every CHI-D case compared to age-matched control (Fig. 2B). This increased Ki67 count was particularly noticeable after the first 4 months consistent with maintained proliferation in CHI-D when replication in normal pancreas was declining. The declining proliferation in normal

pancreas during the first year was largely in acinar cells (Fig. 3A-B). Very little proliferation in α-cells and β-cells was detected beyond 1 year of age. Only two of five cases studied (CHI-D 1 and CHI-D 9) showed elevated β-cell proliferation compared to their controls, the same proportion of specimens with increased α-cell proliferation (CHI-D 1 and CHI-D 2) (Fig. 3C). In contrast, four of the five cases showed increased duct cell proliferation (5 to 11-fold), while all five cases demonstrated increased acinar cell proliferation, which was progressively more noticeable with age. Apoptosis by TUNEL appeared negligible in exocrine tissue and α-cells. As found by Kassem and colleagues (6) apoptosis in β-cells was increased (Fig. 3D), raising the question of whether Ki67 truly reflected cell proliferation or, potentially, DNA damage with attempted repair. As an additional marker of proliferation analysed in >100,000 cells we found phosphohistone H3 (PHH3)-positive cells were on average 5-fold more prevalent in CHI-D (n=2 cases) than in age-matched controls (n=2 cases) and most prevalent in acinar cells (Supplementary Fig. 6); similar to the data on Ki67 [Fig. 2B(i)]. Also, we found no evidence for co-localization of phospho-γ-H2AX (marker of DNA damage) with Ki67-positive cells. Furthermore, *INSULIN* expression was equivalent between CHI-D and controls (Fig. 1B) and the surface area of insulin staining was statistically unchanged between CHI-D [4.9±0.37% (mean±S.E.M.) of sections; 2-13 months, n=5] and age-matched controls (5.8±0.38%; 1-10 months, n=4). These multiple strands of evidence imply no increase of β-cell mass in CHI-D, but predominant proliferation in exocrine cells.

Nuclear CDK6 and P27 in CHI-D

G1/S cell cycle molecules (e.g. CDK6) tend to be cytoplasmic in adult human β-cells (17-19) but upon forced nuclear translocation, can drive proliferation (17; 18). CDK6 staining was predominantly cytoplasmic in control β-cells at 2-3 months with very occasional cells including nuclear localization (Fig. 4A, arrowhead). Staining in fetal β-cells was similarly cytoplasmic at 15 wpc (Fig. 4B). In contrast, cytoplasmic CDK6 was less noticeable in CHI-D β-cells but clearly

nuclear in a proportion (Fig. 4C-D). CDK6 was also nuclear in many CHI-D CK19-positive duct cells (Fig. 4D) and acinar cells (Fig. 4C).

Based on these findings we generated an interactome model of network clusters derived from a CHI microarray dataset (20) (Supplementary Fig. 7A). 1288 genes were significantly altered ($P<0.05$ by ANOVA), which yielded 140 functional modules. When the gene most centrally associated with each module (Supplementary Fig. 7B) was ranked by its priority score as an index of centrality the module containing *CDKN1B* came third (Supplementary Table 4). *CDKN1B* encodes P27, which can potentially inhibit proliferation or act as a chaperone for entry of the CDK6-cyclin complex into the nucleus (17-19). *CDKN1B* expression was increased almost 8-fold in CHI-D pancreas relative to age-matched control (Fig. 4E). P27 was almost entirely cytoplasmic in postnatal control β-cells but extensively nuclear in CHI-D and fetal β-cells (Fig. 4F-H). P27 was also nuclear in CHI-D duct and acinar cells (Fig. 4I and data not shown). Not all cells with these altered cell-cycle proteins were nucleomegalic (Supplementary Fig. 8).

Discussion

Studying the histopathology of cases of CHI-D is useful as modeling in mice with mutant Abcc8 and Kcnj11 has failed to phenocopy all aspects of the disorder. Here, islet disorganization in CHI-D was consistent with findings in *Abcc8* and *Kcnj11* mutant mice (21; 22). While we did not observe increased PP-cells (12), developmental transcription factors were altered. NKX2.2 helps maintain β-cell identity (23) and mutations cause neonatal diabetes (24). The tendency to increased *NKX2.2* in CHI-D pancreas concurs with low *ARX* expression, which it represses (23), and is consistent with an unexpanded PP-cell population. Although CHI-D δ-cells were sparse (12), they more frequently contained NKX2.2, like fetal δ-cells, and made up 10% of endocrine cells with nucleomegaly. It is difficult to conceive that these two δ-cell alterations are secondary to inappropriate insulin from β-cells, arguing that CHI-D directly affects multiple endocrine lineages in keeping with expression of the K_{ATP} channel subunits in multiple islet cell-types in mouse (22).

Atypical nuclei in β-cells and δ-cells might raise concern over future tumour risk, however, CHI-D is not known to predispose to islet cell tumours. Nevertheless, potential δ-cell immaturity tallies with clinical use of somatostatin analogs to inhibit insulin release in CHI-D (1) reviving the notion that the disorder could be in part a defect of δ-cells (12). In contrast, acinar and duct cells are not known to contain the K_{ATP} channel. Their augmented proliferation might therefore reflect inappropriate local insulin concentrations.

Understanding how human β-cells might be provoked into proliferation is a major therapeutic target in diabetes. CHI-D provides a distinctive opportunity to characterize β-cell proliferation in native human tissue. Our data on CDK6 intracellular localization add new weight to the model that its nuclear exclusion is a major checkpoint for human β-cell replication (10) and support P27 as its potential nuclear chaperone rather than a cell-cycle inhibitor (17).

In summary, we report altered pancreatic transcription factors and cell-cycle proteins in CHI-D. How these features relate to the loss of functional K_{ATP} channels, hypoglycemia and inappropriate insulin release would now be interesting to investigate and could assist longer term care of patients with CHI-D.

Acknowledgements

RJS and BH researched data and wrote the manuscript with MJD and NAH. AAB, AS, ZM, REJ, SAS, RDK, SEC, MN, KEC and KPH researched data, reviewed and edited the manuscript. NAH, RDK, PVJ, IB and MJD oversaw tissue collection. This work was supported by the Wellcome Trust (NAH, WT088566MA and WT097820MF), the Medical Research Council (RJS, PhD student, and REJ, clinical fellow), and the National Institute for Health Research (MJD, IB, KEC). Special thanks go to Roger Meadows for help with the microscopy and image analysis. The authors are grateful to research nurses and clinical colleagues at Central Manchester University Hospitals NHS

Trust and the Manchester Biomedical Research Centre. There are no conflicts of interest. NAH is guarantor and takes responsibility for the probity of the data and its analysis.

References

1. Glaser B: Lessons in human biology from a monogenic pancreatic β cell disease. J Clin Invest 2011;121:3821-3825

2. Dunne MJ, Cosgrove KE, Shepherd RM, Aynsley-Green A, Lindley KJ: Hyperinsulinism in infancy: from basic science to clinical disease. Physiol Rev 2004;84:239-275

3. Kapoor RR, Flanagan SE, Arya VB, Shield JP, Ellard S, Hussain K: Clinical and molecular characterisation of 300 patients with congenital hyperinsulinism. Eur J Endocrinol 2013;168:557-564

4. Snider KE, Becker S, Boyajian L, Shyng SL, MacMullen C, Hughes N, Ganapathy K, Bhatti T, Stanley CA, Ganguly A: Genotype and phenotype correlations in 417 children with congenital hyperinsulinism. J Clin Endocrinol Metab 2013;98:E355-363

5. Ashcroft FM, Rorsman P: K-ATP channels and islet hormone secretion: new insights and controversies. Nature Reviews Endocrinology 2013;9:660-669

6. Kassem SA, Ariel I, Thornton PS, Scheimberg I, Glaser B: Beta-cell proliferation and apoptosis in the developing normal human pancreas and in hyperinsulinism of infancy. Diabetes 2000;49:1325-1333

7. Sempoux C, Guiot Y, Dubois D, Nollevaux MC, Saudubray JM, Nihoul-Fekete C, Rahier J: Pancreatic B-cell proliferation in persistent hyperinsulinemic hypoglycemia of infancy: an immunohistochemical study of 18 cases. Mod Pathol 1998;11:444-449

8. Lovisolo SM, Mendonça BB, Pinto EM, Manna TD, Saldiva PH, Zerbini MC: Congenital hyperinsulinism in Brazilian neonates: a study of histology, KATP channel genes, and proliferation of β cells. Pediatr Dev Pathol 2010;13:375-384

9. Dadon D, Tornovsky-Babaey S, Furth-Lavi J, Ben-Zvi D, Ziv O, Schyr-Ben-Haroush R, Stolovich-Rain M, Hija A, Porat S, Granot Z, Weinberg-Corem N, Dor Y, Glaser B: Glucose metabolism: key endogenous regulator of beta-cell replication and survival. Diabetes Obes Metab 2012;14 Suppl 3:101-108

10. Fiaschi-Taesch NM, Kleinberger JW, Salim FG, Troxell R, Wills R, Tanwir M, Casinelli G, Cox AE, Takane KK, Scott DK, Stewart AF: Human pancreatic beta-cell G1/S molecule cell cycle atlas. Diabetes 2013;62:2450-2459

11. Stewart AF: Betatrophin versus bitter-trophin and the elephant in the room: time for a new normal in beta-cell regeneration research. Diabetes 2014;63:1198-1199

12. Rahier J, Falt K, Muntefering H, Becker K, Gepts W, Falkmer S: The basic structural lesion of persistent neonatal hypoglycaemia with hyperinsulinism: deficiency of pancreatic D cells or hyperactivity of B cells? Diabetologia 1984;26:282-289

13. Salisbury RJ, Blaylock J, Berry AA, Jennings RE, De Krijger R, Piper Hanley K, Hanley NA: The window period of NEUROGENIN3 during human gestation. Islets 2014;6:e954436

14. Jennings RE, Berry AA, Kirkwood-Wilson R, Roberts NA, Hearn T, Salisbury RJ, Blaylock J, Piper Hanley K, Hanley NA: Development of the human pancreas from foregut to endocrine commitment. Diabetes 2013;62:3514-3522

15. Piper K, Brickwood S, Turnpenny LW, Cameron IT, Ball SG, Wilson DI, Hanley NA: Beta cell differentiation during early human pancreas development. J Endocrinol 2004;181:11-23

16. Suchi M, Thornton PS, Adzick NS, MacMullen C, Ganguly A, Stanley CA, Ruchelli ED: Congenital hyperinsulinism: intraoperative biopsy interpretation can direct the extent of pancreatectomy. Am J Surg Pathol 2004;28:1326-1335

17. Fiaschi-Taesch NM, Kleinberger JW, Salim FG, Troxell R, Wills R, Tanwir M, Casinelli G, Cox AE, Takane KK, Srinivas H, Scott DK, Stewart AF: Cytoplasmic-nuclear trafficking of G1/S cell cycle molecules and adult human beta-cell replication: a revised model of human beta-cell G1/S control. Diabetes 2013;62:2460-2470

18. Fiaschi-Taesch NM, Salim F, Kleinberger J, Troxell R, Cozar-Castellano I, Selk K, Cherok E, Takane KK, Scott DK, Stewart AF: Induction of human beta-cell proliferation and engraftment using a single G1/S regulatory molecule, cdk6. Diabetes 2010;59:1926-1936

19. Kulkarni RN, Mizrachi EB, Ocana AG, Stewart AF: Human beta-cell proliferation and intracellular signaling: driving in the dark without a road map. Diabetes 2012;61:2205-2213

20. Michelsen NV, Brusgaard K, Tan Q, Thomassen M, Hussein K, Christesen HT: Investigation of Archived Formalin-Fixed Paraffin-Embedded Pancreatic Tissue with Whole-Genome Gene Expression Microarray. ISRN Pathology 2011;2011:Article ID 275102

21. Seghers V, Nakazaki M, DeMayo F, Aguilar-Bryan L, Bryan J: Sur1 knockout mice. A model for K(ATP) channel-independent regulation of insulin secretion. J Biol Chem 2000;275:9270-9277

22. Seino S, Iwanaga T, Nagashima K, Miki T: Diverse roles of K(ATP) channels learned from Kir6.2 genetically engineered mice. Diabetes 2000;49:311-318

23. Papizan JB, Singer RA, Tschen SI, Dhawan S, Friel JM, Hipkens SB, Magnuson MA, Bhushan A, Sussel L: Nkx2.2 repressor complex regulates islet beta-cell specification and prevents beta-to-alpha-cell reprogramming. Genes Dev 2011;25:2291-2305

24. Flanagan SE, De Franco E, Lango Allen H, Zerah M, Abdul-Rasoul MM, Edge JA, Stewart H, Alamiri E, Hussain K, Wallis S, de Vries L, Rubio-Cabezas O, Houghton JA, Edghill EL, Patch AM, Ellard S, Hattersley AT: Analysis of transcription factors key for mouse pancreatic development establishes NKX2-2 and MNX1 mutations as causes of neonatal diabetes in man. Cell Metab 2014;19:146-154

Figure Legends

Figure 1. Expression of key transcription factors in CHI-D pancreas

(A) qRT-PCR analysis of *NEUROG3* in triplicate in CHI-D1 and CHI-D2 and age-matched controls (mean +/- S.E.M.) standardized against levels of detection in the human fetal pancreas at 14 wpc. **(B)** qRT-PCR analysis of eleven transcription factors and insulin. Data from each CHI-D sample were performed in triplicate and standardized against their own age-matched control, prior to displaying data as mean levels (+/- S.E.M.) for all CHI-D samples. **P*<0.01 following Hochberg correction. **(C)** qRT-PCR expression for *NKX2.2* in samples of CHI-D (performed in triplicate; mean +/- S.E.M.) during the first six months compared to their age-matched control. **(D)** Cell counting of dual immunofluorescence for NKX2.2 with islet hormones, insulin (INS), glucagon (GLU), somatostatin (SS) and ghrelin (GHREL) for the four CHI-D samples in **(C)**, their age-matched controls and human fetal pancreas (two specimens at 11 and 15 wpc). Data are expressed as the mean (+/- S.E.M.) percentage for each hormone lineage. NKX2.2 is retained in somatostatin-positive CHI-D cells compared to the age-matched controls (**P*<0.01). **(E)** Examples (as counted in **C**) of dual immunofluorescence for somatostatin (SS) and NKX2.2 counterstained with DAPI. Arrows show colocalization in fetal and CHI-D samples. Scale bar represents 10 μm.

Figure 2. Cell proliferation is increased in CHI-D tissue

(A) Proliferation in human control pancreas from 10 weeks post-conception (wpc), during the first year after birth (weeks, months), and >12 years. All data points have been gathered from individual cases, except for the data associated with ≥12 years which is averaged data from n=4 cases. Proliferation has been assessed by high-density counting from a minimum of 20,000 cells with $Ki67^+$ cells expressed as a percentage of the total cell count. (i)-(iv) representative images from fetal tissue at 18 wpc, and postnatal pancreas at 10 weeks and 10 months. $Ki67^+$ cells are stained brown and are clearly seen in islets; arrows in panel (iv). Scale bars represent 100 μm in (i)-(iii) and 50 μm in (iv). **(B)** Proliferation in CHI-D tissue. (i) Average fold increase in Ki67 count expressed relative to age-matched control from cases up to 4 months and the older ones. (ii) Individual data from the nine cases compared to age-matched controls demonstrate particularly higher proliferation rates at older ages. C, age-matched control; #, patient identifier.

Figure 3. Increased proliferation in all pancreatic cell lineages in CHI-D tissue

(A) Dual immunofluorescence of markers for endocrine cells (β-cells, insulin; α-cells, glucagon) and non-endocrine cells (duct cells, SOX9; and acinar cells, GATA4) (green) in the pancreas with Ki67 (red) for CHI-D pancreas, postnatal control tissue and an example of fetal tissue at 14 wpc. Arrows show examples of co-stained cells. Scale bar represents 20 μm for all panels. **(B)** Total counts (+/- S.E.M.) for $Ki67^+$ cells dual stained for the markers of different pancreatic lineages in human control pancreas. Total Ki67 count correlated inversely with age, (r^2=-0.929, P<0.01). **(C)** Fold increase (+/- S.E.M.) in proliferation for each cell lineage (as defined by the markers in A) for each CHI-D sample compared to its age-matched control. Each bar stacks the fold increments for each cell lineage. **(D)** Relative counts (+/- S.E.M.) for $TUNEL^+$/$Insulin^+$ cells expressed as a percentage of the total insulin-positive cells for fetal, CHI-D and their age-matched postnatal controls. Statistical analysis performed using Mann-Whitney U test; **P*<0.05, ***P*<0.01.

Figure 4. Increased nuclear localization of CDK6 and P27 in CHI-D

Brightfield immunohistochemistry counterstained with toluidine blue and dual immunofluorescence counterstained with DAPI for CDK6 (**A-D**) or P27 (**F-I**) in postnatal control pancreas, examples of fetal pancreas and CHI-D. Costaining is with insulin apart from examples with CK19 in **D** and **I**. Hatched lines in the brightfield images encircle islets. **A-D.** Arrowhead in the merged panel of **A** points to insulin-positive cells, in which CDK6 localizes to both cytoplasm and nucleus. In **C** the cytoplasmic CDK6 is very much reduced in CHI-D compared to control or fetal β-cells while the arrow in the merged panel (and arrows in **D.**) points to clear nuclear CDK6 in insulin-positive cells. **E.** qRT-PCR showing increased *CDKN1B* expression in CHI-D (mean +/- S.E. from five cases across the first 13 months of age) compared to age-matched controls (n=3). *, $P<0.05$ by Mann-Whitney U test. **F-I.** P27 is almost exclusively cytoplasmic in postnatal control β-cells while it is almost exclusively nuclear in fetal and CHI-D β-cells, and in CK-19-positive duct cells. Scale bars represent 50 μm (**A, C**), 20 μm (**B**) and 10 μm (**D**, **F-I**).

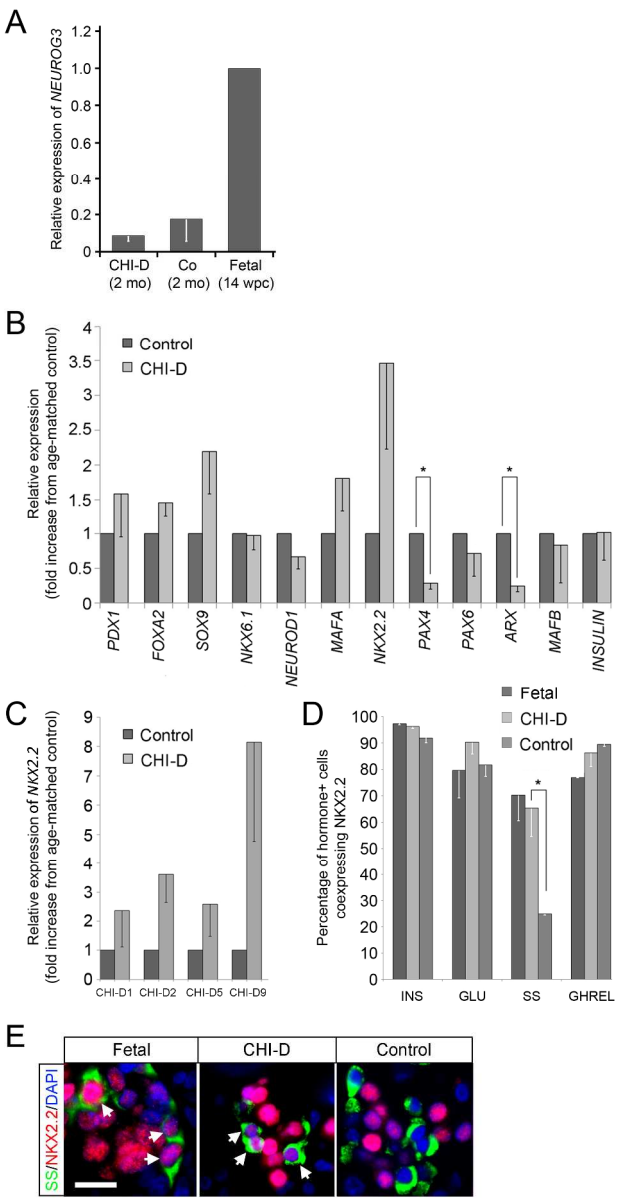

Fig 1
179x345mm (300 x 300 DPI)

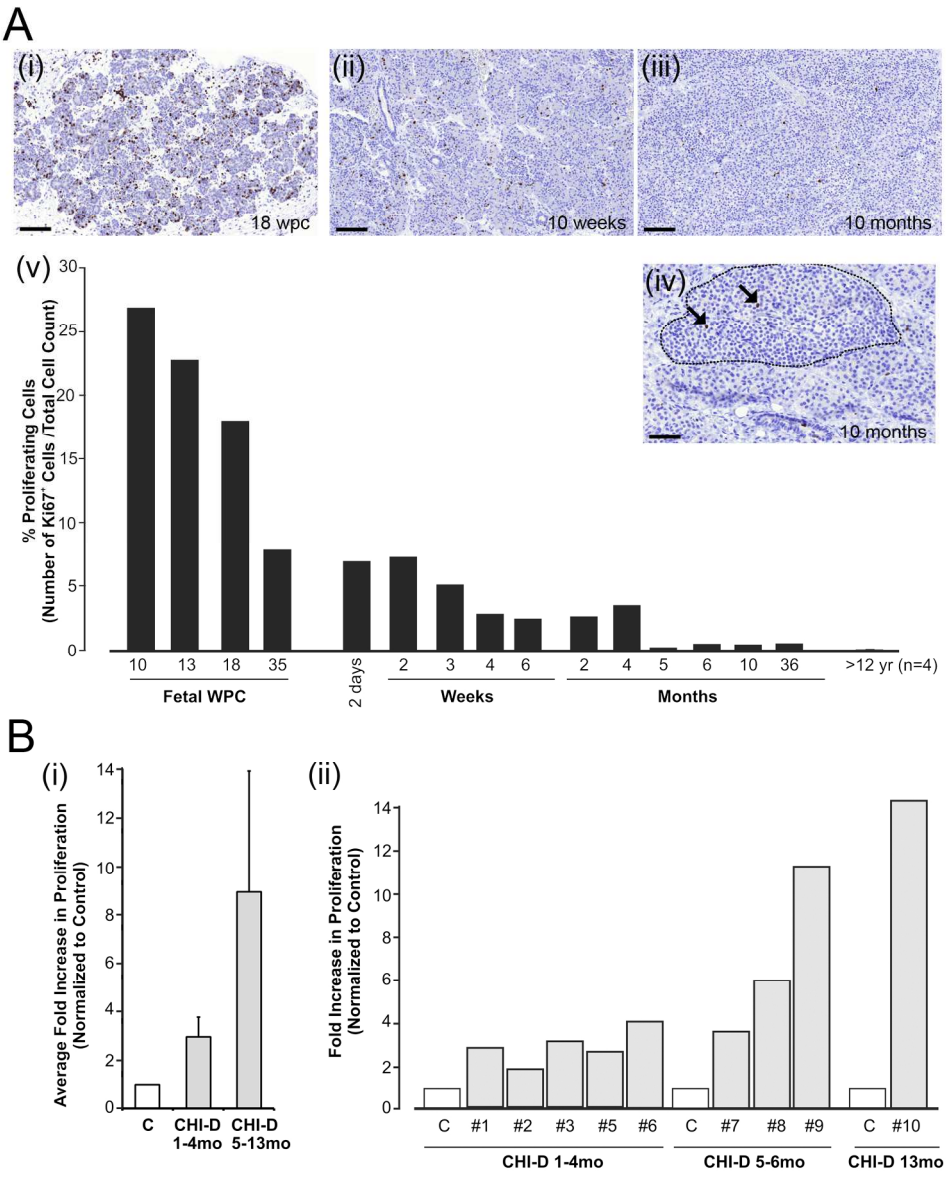

Figure 2
180x225mm (300 x 300 DPI)

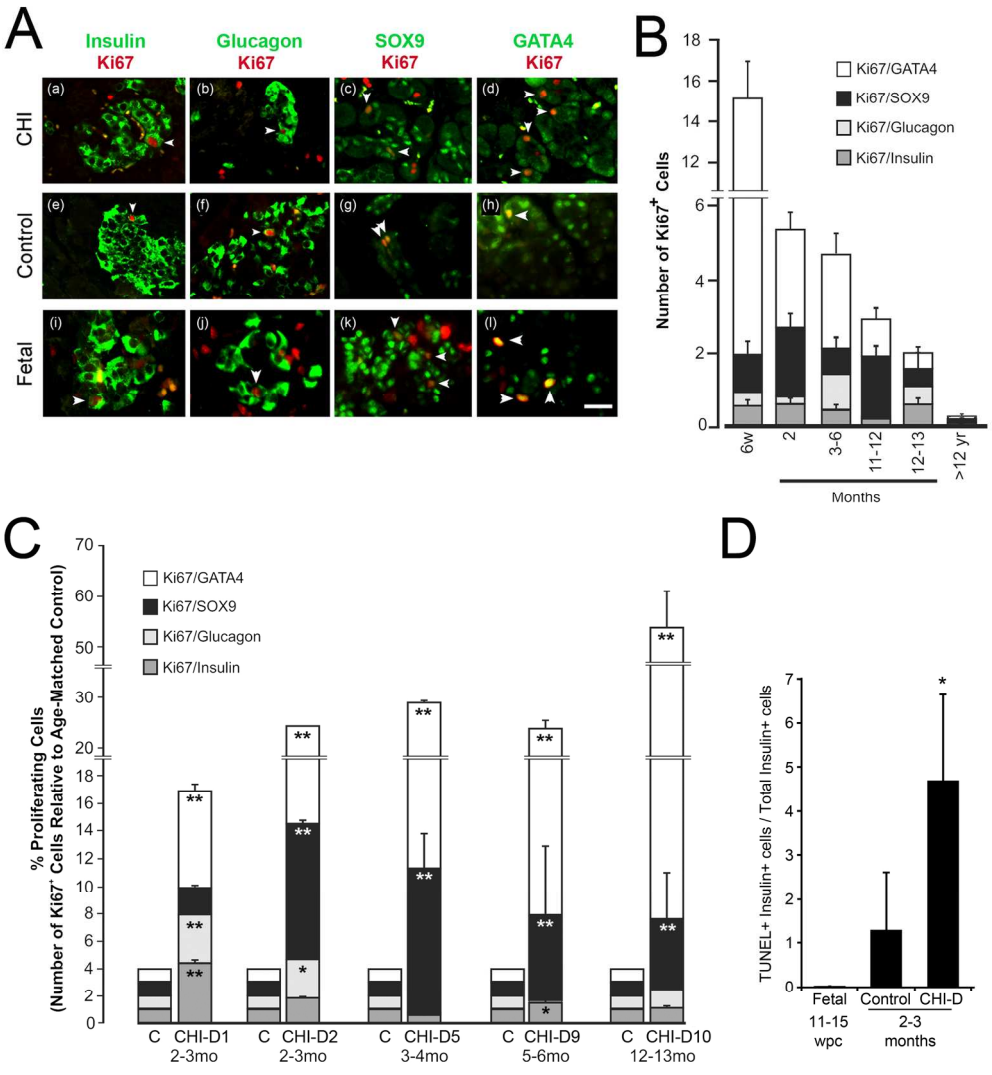

Fig 3
196x214mm (300 x 300 DPI)

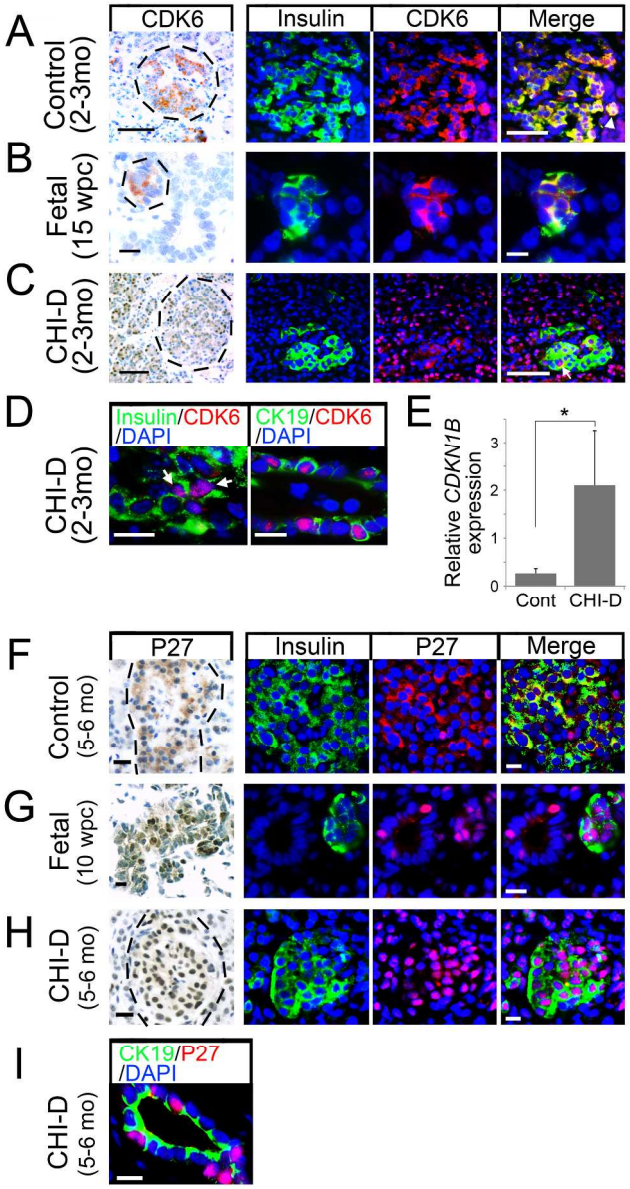

Figure 4
168x319mm (300 x 300 DPI)

Online appendix for Salisbury et al, DB14-1202

Methods for data shown in the Online Appendix

Gene expression, pathway and network analyses

Gene expression associated with CHI-D was determined using GSE32610 from the Gene Expression Omnibus (GEO: http://www.ncbi.nlm.nih.gov/geo/) (1). The transcriptomic datasets of CHI and control pancreas [Human 58K oligonucleotide array (GPL14670)] were downloaded into Qlucore Omics Explorer 2.3 (Qlucore, Lund, Sweden), normalized by multi-dimensional scaling (Isomapping) (2) and compared by ANOVA with a significance cut-off of $P<0.05$. Identification of biological pathways and functions associated with gene expression changes was undertaken using a right-sided Fisher's exact test within Ingenuity Pathway Analysis (IPA) software. Network analysis was also used to identify and prioritize key functional elements. In brief, to derive an interactome model differentially expressed genes were used as 'seeds' and all known protein:protein and protein:gene interactions between the seeds and their inferred immediate neighbours were calculated to generate a biological network using the Biogrid model of the human Interactome (31.2.101) (3). Network generation and processing was performed using Cytoscape 2.8.3. Clustering and 'community structure' within interactome models, known to be associated with function (4-6), was prioritized using the ModuLand plug-in for Cytoscape 2.8.3 to determine overlapping modules (7) and to identify hierarchical structure (8). Clusters were confirmed using MCODE algorithm (9) and module centrality was used to derive a priority index for genes of biological importance.

Supplementary references

1. Michelsen NV, Brusgaard K, Tan Q, Thomassen M, Hussein K, Christesen HT: Investigation of Archived Formalin-Fixed Paraffin-Embedded Pancreatic Tissue with Whole-Genome Gene Expression Microarray. ISRN Pathology 2011;2011:Article ID 275102
2. Tenenbaum JB, de Silva V, Langford JC: A global geometric framework for nonlinear dimensionality reduction. Science 2000;290:2319-2323
3. Chatr-Aryamontri A, Breitkreutz BJ, Heinicke S, Boucher L, Winter A, Stark C, Nixon J, Ramage L, Kolas N, O'Donnell L, Reguly T, Breitkreutz A, Sellam A, Chen D, Chang C, Rust J, Livstone M, Oughtred R, Dolinski K, Tyers M: The BioGRID interaction database: 2013 update. Nucleic Acids Res 41:D816-823
4. Sun J, Zhao Z: A comparative study of cancer proteins in the human protein-protein interaction network. BMC Genomics 2010;11 Suppl 3:S5
5. Ravasz E, Barabasi AL: Hierarchical organization in complex networks. Phys Rev E Stat Nonlin Soft Matter Phys 2003;67:026112
6. Yu H, Kim PM, Sprecher E, Trifonov V, Gerstein M: The importance of bottlenecks in protein networks: correlation with gene essentiality and expression dynamics. PLoS Comput Biol 2007;3:e59
7. Szalay-Beko M, Palotai R, Szappanos B, Kovacs IA, Papp B, Csermely P: ModuLand plug-in for Cytoscape: determination of hierarchical layers of overlapping network modules and community centrality. Bioinformatics 28:2202-2204
8. Kovacs IA, Palotai R, Szalay MS, Csermely P: Community landscapes: an integrative approach to determine overlapping network module hierarchy, identify key nodes and predict network dynamics. PLoS One 2010;5
9. Bader GD, Hogue CW: An automated method for finding molecular complexes in large protein interaction networks. BMC Bioinformatics 2003;4:2
10. Piper K, Brickwood S, Turnpenny LW, Cameron IT, Ball SG, Wilson DI, Hanley NA: Beta cell differentiation during early human pancreas development. J Endocrinol 2004;181:11-23

Supplementary tables

Patient	Age at Surgery	Sex	Birth Weight (kg)	Gene Defect	Inheritance AD/AR	Paternal Mutation	Maternal Mutation
CHI-D1	2m	M	6.7	*ABCC8*	AR	p.? (c.3992-9G>A)	p.? (c.3992-9G>A)
CHI-D2	2m	M	4.3	*KCNJ11*	AR	p.Q299R (c.896A>G)	p.Q299R (c.896A>G)
CHI-D3	2m	M	4.4	*ABCC8*	AR	p.A30V (c.89C>T)	p.A30V (c.89C>T)
CHI-D4	2m	F	3.5	*ABCC8*	AR	p.S581T (c.1741T>A)	p.? (c.3992-9G>A)
CHI-D5	3m	M	4.5	*ABCC8*	AR	p.? (c.1818-?_1923+?del)	p.T172fs c.512dup
CHI-D6	4m	M	2.9	*ABCC8*	AR	p.H36R (c.107A>G)	p. ? (c.1630+1G>T)
CHI-D7	5m	M	3.5	*ABCC8*	AR	p.L610P (C.1829T>C)	p.L610P (C.1829T>C)
CHI-D8	5m	M	1.9	*ABCC8*	AD	p.I1512T (c.4535T>C)	-
CHI-D9	6m	M	2.9	*ABCC8*	AR	p.? (c.148+1G>A)	p.? (c.148+1G>A)
CHI-D10	13m	F	4.6	*ABCC8*	AR	p.? (c.4612-1G>T)	p.A4V (c.11C>T)

Supplementary Table 1. CHI-D patient information. Ten cases undergoing pancreatectomy for sustained hypoglycemia unresponsive to medical treatment. Mode of inheritance for gene defects; AR=autosomal recessive, AD=autosomal dominant. Details of mutations; p.? = intronic mutation resulting in unknown protein size.

Primary Antibody	Raised In	Dilution	Supplier
Polyclonal anti-insulin	Rabbit	1:1000	Abcam
Polyclonal anti-insulin	Guinea Pig	1:100	Zymed
Polyclonal anti-glucagon	Rabbit	1:50	Zymed
Polyclonal anti-somatostatin	Rabbit	1:50	Zymed
Polyclonal anti-PP	Rabbit	1:50	Zymed
Polyclonal anti-ghrelin	Goat	1:500	Abcam
Polyclonal anti-gastrin	Rabbit	1:200	Cell Marque
Monoclonal anti-NKX6.1	Mouse	1:1000	DSHB
Monoclonal anti-NKX2.2	Mouse	1:75	DSHB
Monoclonal anti-Ki67	Mouse	1:100	Novocastra
Monoclonal anti-PHH3	Mouse	1:200	Cell Signaling
Polyclonal anti-phospho-γ-H2AX	Rabbit	1:200	Cell Signaling
Polyclonal anti-SOX9	Rabbit	1:5000	Millipore
Polyclonal anti-GATA4	Goat	1:450	Abcam
Polyclonal anti-CDK6	Rabbit	1:500	Abcam
Polyclonal anti-CK19	Mouse	1:100	Novocastra
Polyclonal anti- P27Kip1	Rabbit	1:200	Santa Cruz
Polyclonal anti-pRb	Rabbit	1:500	Abcam
Polyclonal anti-FOXA2	Goat	1:800	R & D
Polyclonal anti-PDX1	Guinea pig	1:500	Abcam
Monoclonal anti-ISL1	Mouse	1:200	DSHB

Supplementary Table 2. Primary antibodies

The antibodies developed by O.D. Madsen (anti-NKX6.1) and T.M. Jessell (anti-NKX2.2 and anti-ISL1) were obtained from the Developmental Studies Hybridoma Bank developed under the auspices of the NICHD and maintained by the University of Iowa, Department of Biology, Iowa City, IA 52242.

Gene	Accession No.	Forward Primer	Reverse Primer	Size (bp)
β-ACTIN	NM_001101.3	CCAACCGCGAGAAGATGA	CCAGAGGCGTACAGGGATAG	138
HPRT	NM_000194.2	TGACCTTGATTTATTTTGCATACC	CGAGCAAGACGTTCAGTCCT	102
PDX1	NM_000209.3	AAAGGCCAGTGGGCAGGCGG	GCGCGGCCGTGAGATGTACT	135
FOXA2	NM_021784.4	GAAGATGGAAGGGCACGAGC	GTACGTGTTCATGCCGTTCA	115
SOX9	NM_000346.3	GTACCCGCACTTGCACAAC	TCGCTCTCGTTCAGAAGTCTC	72
NKX6.1	NM_006168.2	GGCCTGTACCCCTCATCAAG	TCCGGAAAAAGTGGGTCTCG	79
NEUROD1	NM_002500.4	GAGGCCCCAGGGTTATGAGA	TGGTCATGTTTCGATTTCCTTTGT	70
MAFA	NM_201589.3	AGAGCGAGAAGTGCCAACTC	GTACAGGTCCCGCTCTTTGG	83
NKX2.2	NM_002509.3	ATGTCGCTGACCAACACAAAG	GATGTCCTTGACCGAAAACCC	45
INSULIN	NM_001185097.1	TGGCTTCTTCTACACACCCA	TCTAGTTGCAGTAGTTCTCCA	984
PAX4	NM_006193.1	AAGAAAGCAGCTTGCGTTGAC	GGGCGTGAGACAGAGGTATC	165
PAX6	NM_000280.4	CCCGGCAGAAGATTGTAGAG	GCTAGCCAGGTTGCGAAGAA	323
ARX	NM_139058.2	ATTCGGCAGGCTCTTTTCCA	ATGTTGGAGTTGGAGCGAGG	502
MAFB	NM_005461.3	TGAACTTTGCGCGTTAAGCC	CACGCAGCCGCCGGAGTTTC	436
CDKN1B	NM_004064.4	TCCGGCTAACTCTGAGGACA	GAAGAATCGTCGGTTGCAGG	120

Supplementary Table 3. qRT-PCR primers

Forward and reverse primer sequences are given for each gene along with the accession number and product size. All primer pairs / products were intron-spanning wherever possible.

Module rank	**Most central gene in the module** (others genes in the top 10)
1	***EP300*** (*UBD, SIRT7, KAT2B, TP53, FN1, PRMT1, ARRB1, VCAM1, TRIM28*)
2	***PML*** (*UBD, DAXX, SUMO2, TRIM28, FN1, SUMO1, PIAS1, ARRB1, VCAM1*)
3	***CDKN1B*** (*CDK2, CDK7, CDK4, SKP2, CCT8, UBD, CCNE1, COPS5, VCAM1*)
4	***NCOA2*** (*ESR1, EP300, AR, GNAI2, PRMT1, FN1, SIRT7, SAFB, ACTR2*)
5	***CAND1*** (*CUL1, COPS3, FN1, CUL3, PHKG2, CUL4A, RNF7, SIRT7, UBD*)
6	***PIK3R1*** (*CRK, FYN, CBL, VAV1, ITSN1, ERBB3, GRB2, EGFR, BCAR1*)
7	***TBP*** (*TAF9, TAF6, TAF10, TAF5, TCEA1, TAF1, TAF4, ELAVL1, GTF2B*)
8	***HDAC5*** (*AR, UBD, TBL1XR1, NCOR1, PHKG2, ZBTB16, ARRB1, HNF4A, HSP90AA1*)
9	***CDK7*** (*TCEA1, CCNH, GTF2H2, POLR2A, SIRT7, ERCC3, MNAT1, GTF2H1, APP*)
10	***COPS3*** (*COPS5, COPS6, ERCC8, TK1, SIRT7, CUL3, DDB1, CUL4B, TOR1AIP2*)
11	***MRE11A*** (*SIRT7, RAD50, NBN, DDX1, TERF1, BRCA1, NRF1, HNRNPD, VCAM1*)
12	***ZBTB16*** (*HDAC1, HDAC5, TRIM28, FN1, PHB, DNMT3B, TK1, EHMT2, VCAM1*)
13	***SMURF1*** (*SMAD1, SMAD7, SMAD5, STRAP, NEDD4, APP, DCTN2, PHKG2, UBE2D3*)
14	***FN1*** (*SIRT7, HNRNPD, VCAM1, GAPDH, VHL, TK1, PHKG2, CCT8, ELAVL1*)
15	***BAG1*** (*HSPA8, HSPA4, TTC1, ARRB1, NRF1, PHKG2, STUB1, TERF1, ACTR2*)
16	***NEDD4*** (*UBE4B, UBE2D2, UBE2D3, UBE2L3, LAPTM5, MKRN3, MGRN1, ARRB1, UBE2D1*)
17	***UBE2M*** (*APP, NEDD8, PDIA3, NRF1, RBX1, CLU, NDUFS6, DCUN1D1, UBA3*)
18	***PSMA6*** (*PSMA5, UBD, VCAM1, PHKG2, FKBP8, FN1, PSMA2, PSMA3, STK4*)
19	***HEXIM1*** (*BRD4, CDK9, CCNT1, EAF1, TERF1, RN7SK, NRF1MED12, STK4*)
20	***RING1*** (*BMI1, PHC1, RNF2, PCGF2, PHC2, INTS6, CBX4, TERF1, APP*)

Supplementary Table 4. Top 20 functional modules following network analysis ranked by the index of centrality of their most central gene

The most central gene in the top 20 modules is shown in bold. In parentheses are the other genes in the top ten for each module.

Supplementary figures

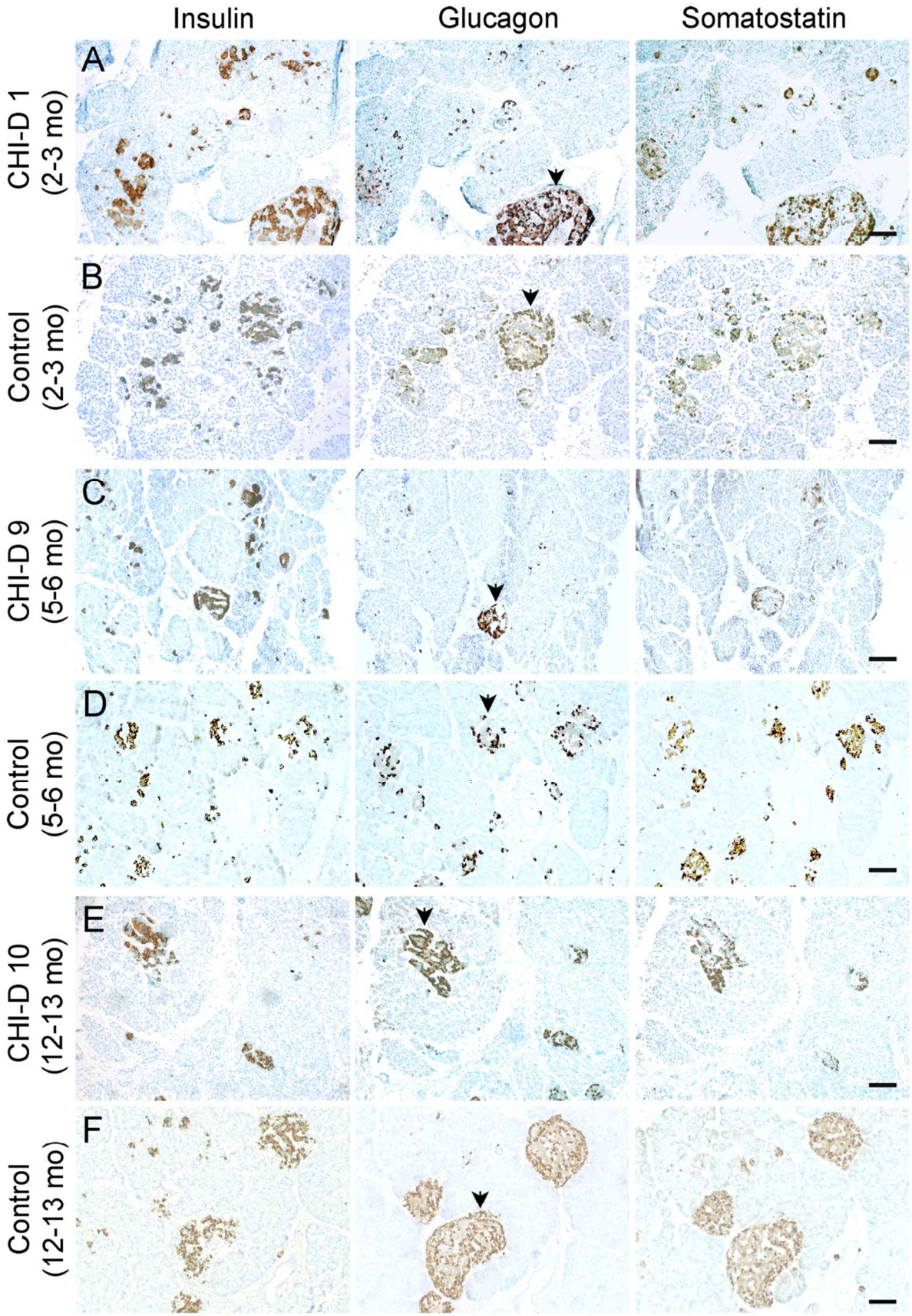

Supplementary Figure 1. β-cells, α-cells and δ-cells in CHI-D and control pancreas during the early postnatal period

Consecutive 5 μm sections from three examples of CHI-D and age-matched control pancreas are stained for insulin (β-cells), glucagon (α-cells) and somatostatin (δ-cells) (all brown) counter-stained with toluidine blue. **(A-B)** 2-3 months (mo); **(C-D)** 5-6 months; and **(E-F)** 12-13 months. Arrowheads in each glucagon panel point to an islet at each age that is also apparent in sections either side stained for insulin and somatostatin. At 2-3 months, note the extra-islet, scattered hormone-positive cells in both CHI-D and controls. At all ages, note that glucagon-positive cells are more evenly distributed throughout the islets in CHI-D compared to the peripheral α-cells in control islets. The consistently central insulin staining and, in older CHI-D samples, more peripheral somatostatin in adjacent sections exemplifies that this feature was not due to the plane of sectioning (also see Fig. 1 in main text). Gastrin was not observed in CHI-D or age-matched control pancreas compared to a positive control of human fetal intestine at 10 weeks post-conception (**image below**). Scale bar represents 200 μm.

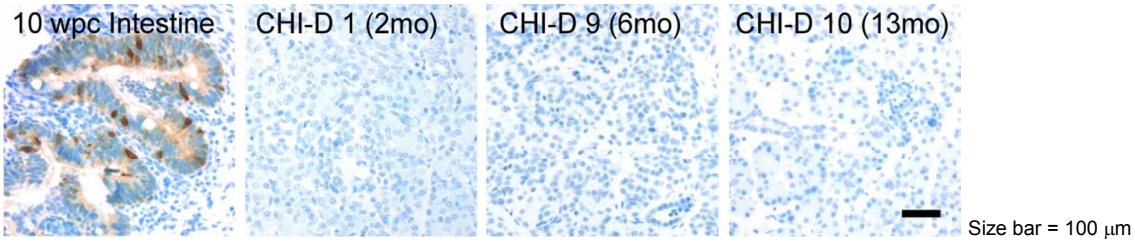

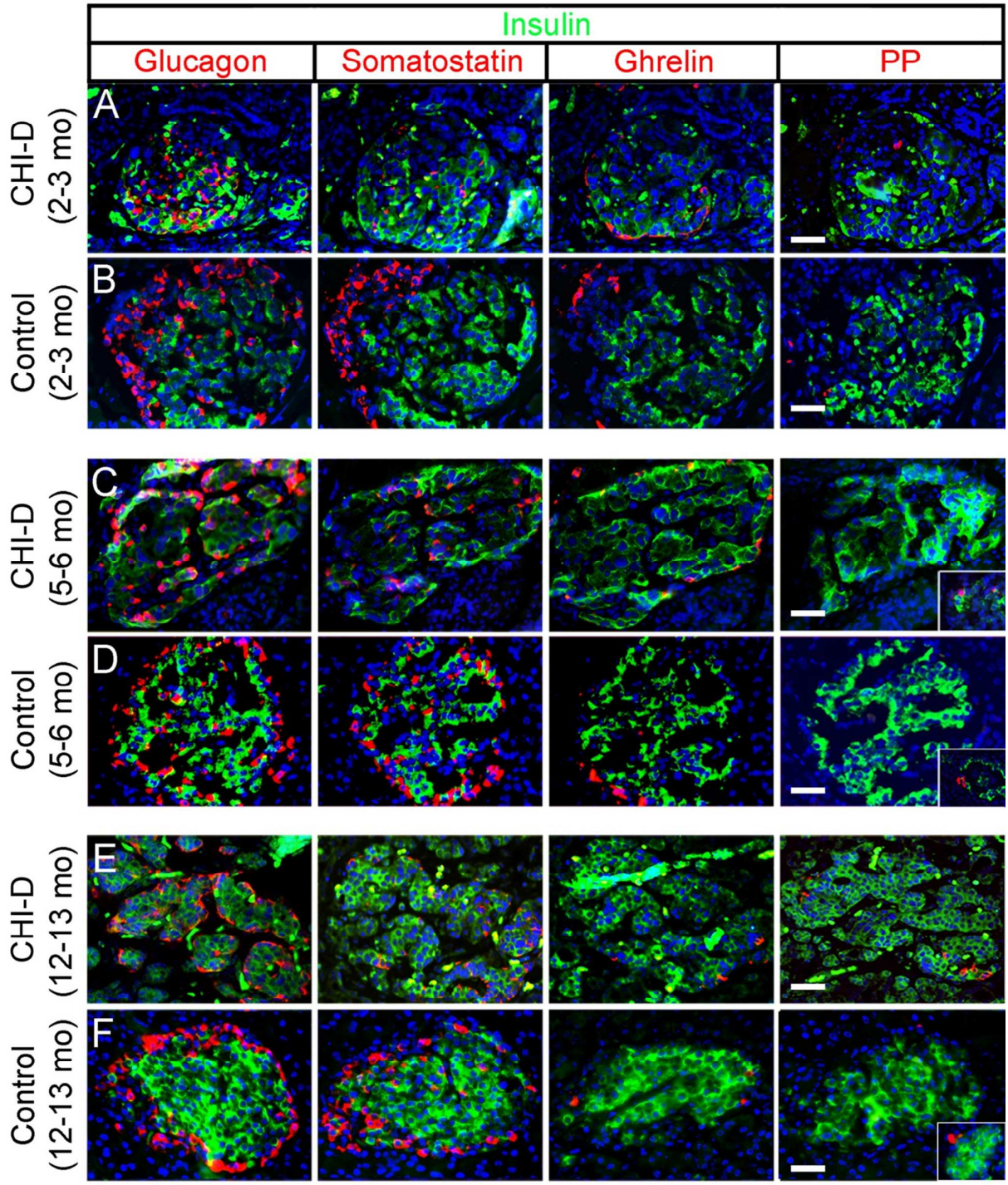

Supplementary Figure 2. Endocrine lineages and islet composition in CHI-D and age-matched controls

Dual confocal immunofluorescence of consecutive sections from CHI-D and age-matched control pancreas counterstained with DAPI. (**A-B**), 2-3 months (mo); (**C-D**), 5-6 months; and **(E-F)**, 12-13 months. Insets demonstrate PP staining elsewhere within the same section. At early stages α-cells and δ-cells are more diffusely scattered throughout islets rather than arranged as a mantle. Ghrelin staining was located peripherally along with occasional PP-cells in both CHI-D and control Islet structure remains less organized and compact in CHI-D. Scale bars represent 100 μm.

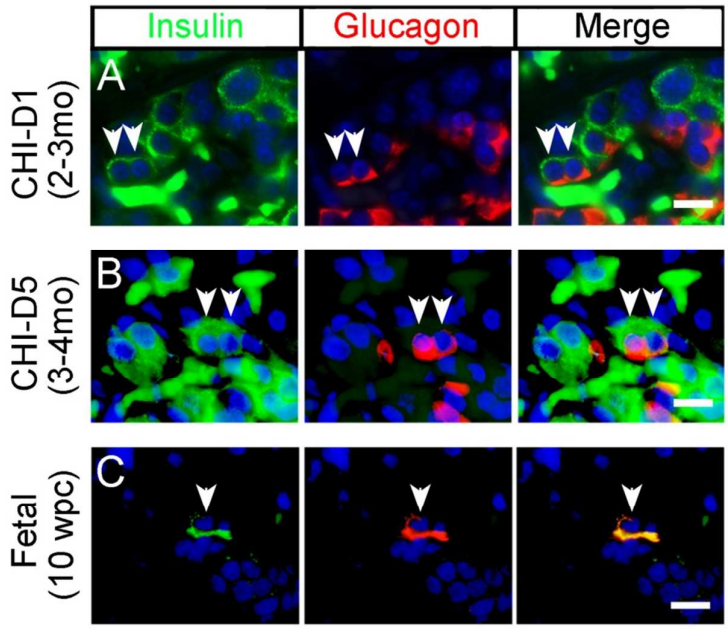

Supplementary Figure 3. Localization of insulin and glucagon within the same endocrine cells in CHI-D

Dual confocal immunofluorescence for insulin and glucagon counterstained with DAPI in tissue sections from two cases of CHI-D **(A-B)** and human fetal pancreas **(C)** at 10 weeks post-conception (wpc). In CHI-D the arrowheads point to cells which contain both insulin and glucagon but where each hormone localizes to a discrete area of the cell. In contrast, detection of the two hormones completely overlaps in human fetal pancreas (10). The associated supplementary video confirms the cellular co-detection by moving through a cell on confocal Z-stack. Scale bar represents 50 μm.

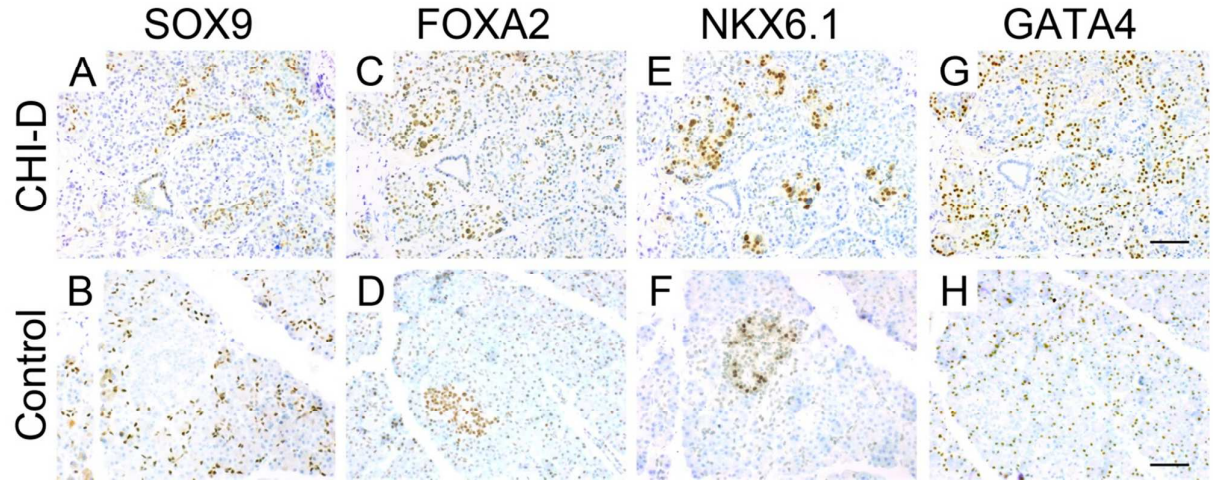

Supplementary Figure 4. SOX9, FOXA2, NKX6.1 and GATA4 in CHI-D and control pancreas

Brightfield immunohistochemistry counterstained with toluidine blue shows SOX9 (duct cells, **A-B**), FOXA2 (duct cells and β-cells**, C-D**), NKX6.1 (β-cells, **E-F**) and GATA4 (acinar cells, **G-H**) in an example of CHI-D pancreas and its aged-matched control. The staining profile was identical in all CHI-D samples (2-13 months). Note examples of nucleomegaly amongst the FOXA2 and NKX6.1 staining in CHI-D but not CHI-D duct or acinar cells or any of the control cells. NKX6.1

also illustrates the diffuse nature of β-cells in CHI-D compared to control pancreas. Note also the increased GATA4 staining in CHI-D compared to control consistent with the major acinar cell proliferation observed in CHI-D (Fig. 6C, main text). Along with satisfactory tissue morphology, the sensitive detection of nuclear transcription factors argues against significant pancreatic autolysis. Scale bars represent 200 μm.

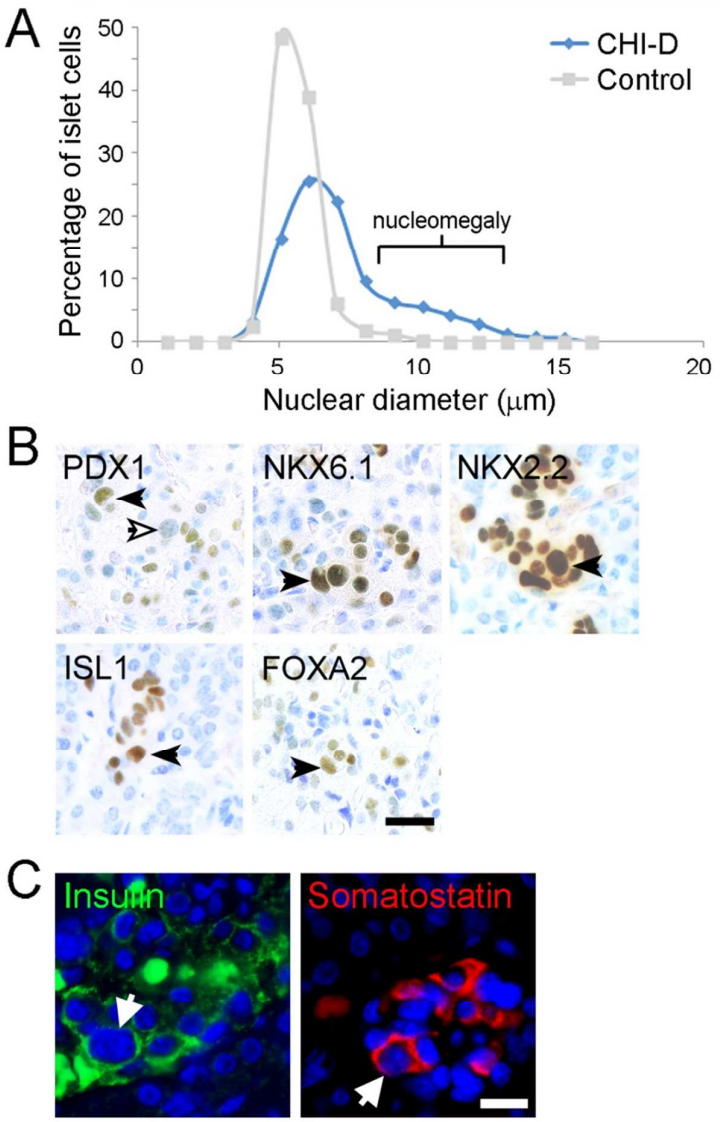

Supplementary Figure 5. Nucleomegaly in CHI-D affects δ-cells as well as β-cells
(A) Nuclear diameter of islet cells in CHI-D samples compared to age-matched controls. CHI-D cells had larger nuclei on average with a subset having especially large nuclei beyond a normal distribution (nucleomegaly; marked on graph). Diameter was measured using digitization data obtained from histological slides using the HistoQuant and Pannoramic Viewer software. **(B)** Brightfield immunohistochemistry for transcription factors (stained brown) in CHI-D pancreas demonstrating examples of nucleomegaly (arrowheads). Not all nucleomegalic cells stained for PDX1 (e.g. white arrowhead). Size bar represents 20 μm. **(C)** Immunofluorescence counterstained with DAPI. Arrows demonstrate examples of nucleomegalic β-cells (stained for insulin) and δ-cells (stained for somatostatin). Scale bar represents 10 μm.

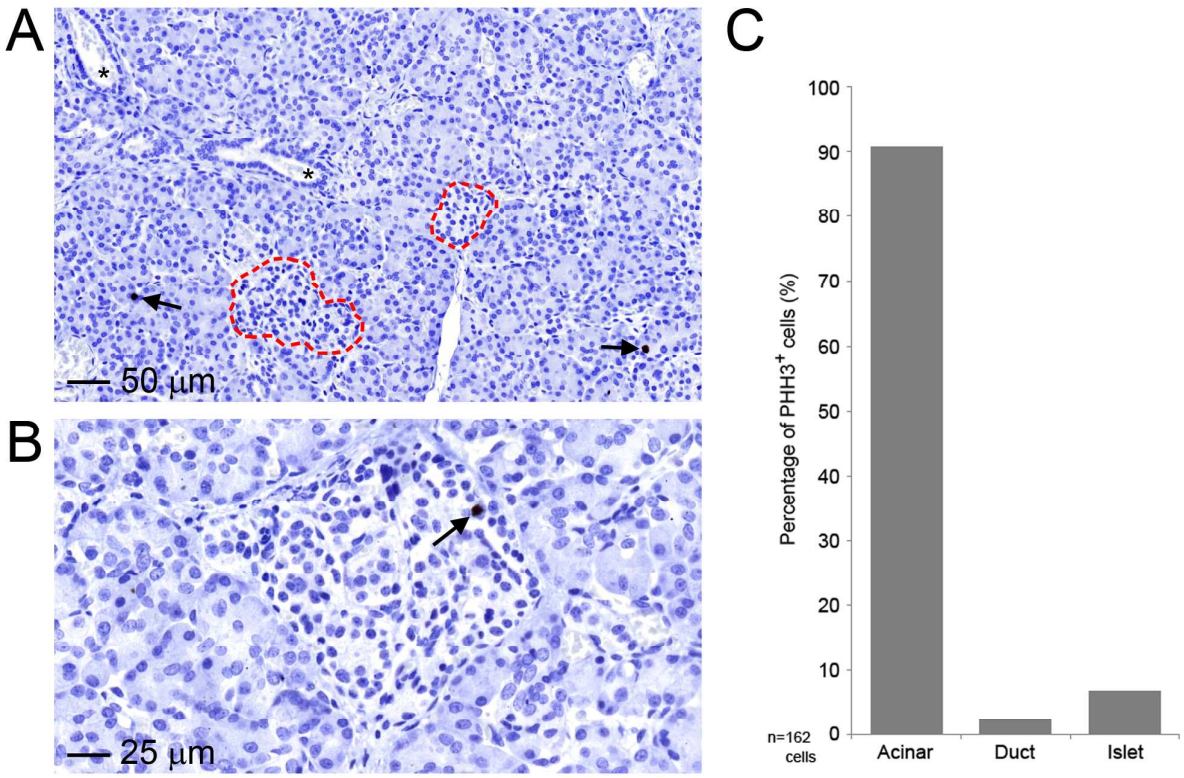

Supplementary Figure 6. Relative detection of PHH3 in CHI-D pancreas.
(A) PHH3 was predominantly detected in acinar cells (arrows), rather than in ducts (asterisk) or islets (red hatched circles). **(B)** Higher magnification example to show PHH3 detection within an islet. **(C)** Summary data of PHH3-positive cells in two cases of CHI-D. Approximately 90% of PHH3-positive cells were acinar, 7% were islet and 3% were duct (n=162).

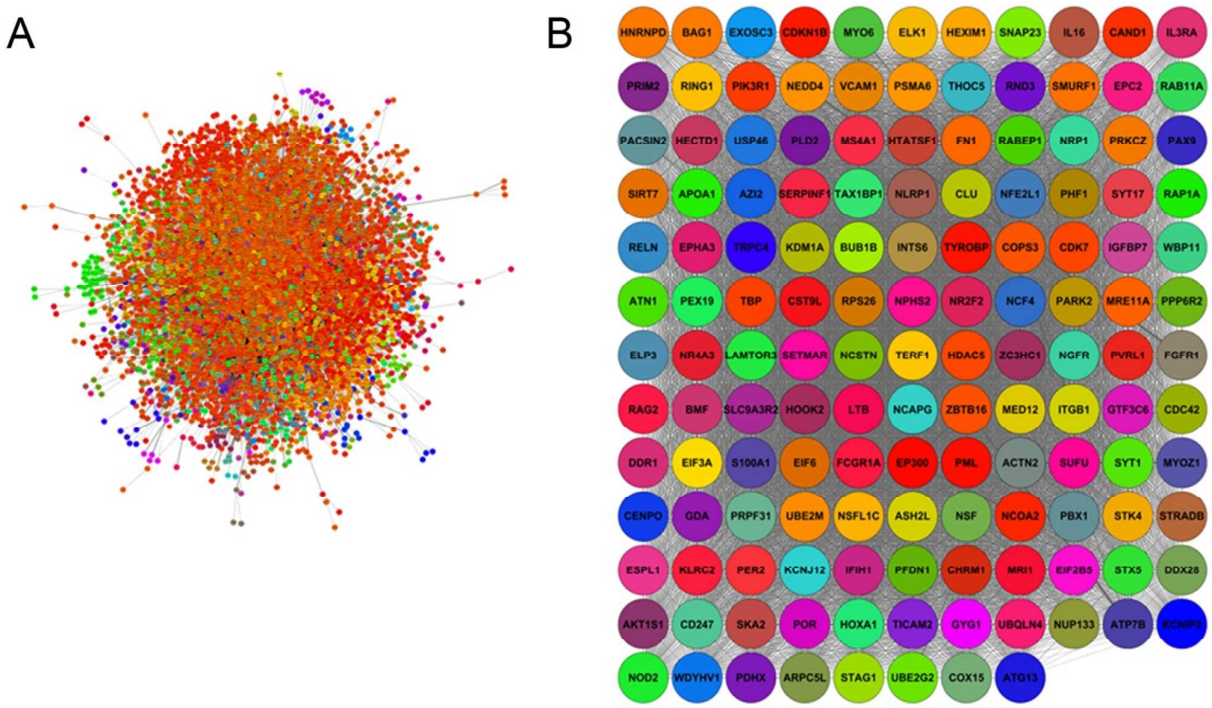

Supplementary Figure 7. Clusters of genes identified as functional modules within a network model of CHI

(A) Interactome model derived from the BioGRID database of significantly altered gene expression in CHI tissue (1). Cluster modules (coloured) were identified with the interactome model using the Moduland algorithm. **(B)** Network of the cluster modules showing the most central gene (top 20 ranking shown in Supplementary Table 4).

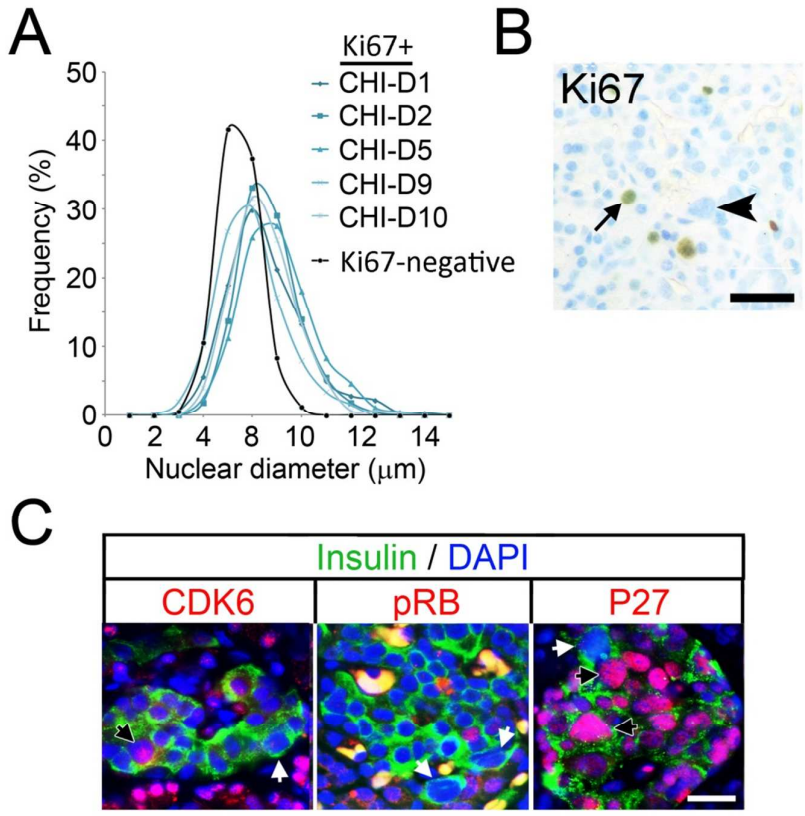

Supplementary Figure 8. Correlation between cell-cycle markers and β-cell nucleomegaly
(A) Ki67-positive nuclei in CHI-D are slightly larger. Frequency histograms showing the range of nuclear diameters recorded in Ki67-positive cells from each of the five cases of CHI-D (blue curves) and the mean diameter from Ki67-negative cells from the same cases (black curve). Comparing nuclear diameter in Ki67-positive and Ki67-negative populations was significant at $P<0.01$. **(B)** Example of nuclear Ki67 staining (arrow) showing not all nucleomegalic cells are proliferative (arrowhead). **(C)** Dual immunofluorescence for CDK6, retinoblastoma protein (pRb) and P27 proteins with insulin counterstained with DAPI showing not all nucleomegalic cells are positively stained. Scale bar represents 20 μm.

Supplementary Video. Insulin and glucagon colocalization in CHI-D
Animation captured at x630 magnification moving through a series of cross-sectional z-stack images for a CHI-D cell demonstrating codetection of insulin (green) and glucagon (red).